A Small-Molecule Inhibitor of Bcl-X_L Potentiates the Activity of Cytotoxic Drugs *In vitro* and *In vivo*

Alex R. Shoemaker,[1] Anatol Oleksijew,[1] Joy Bauch,[1] Barbara A. Belli,[2] Tony Borre,[1] Milan Bruncko,[1] Thomas Deckwirth,[2] David J. Frost,[1] Ken Jarvis,[1] Mary K. Joseph,[1] Kennan Marsh,[1] William McClellan,[1] Hugh Nellans,[1] ShiChung Ng,[1] Paul Nimmer,[1] Jacqueline M. O'Connor,[1] Tilman Oltersdorf,[2] Weiguo Qing,[1] Wang Shen,[1] Jason Stavropoulos,[1] Stephen K. Tahir,[1] Baole Wang,[1] Robert Warner,[1] Haichao Zhang,[1] Stephen W. Fesik,[1] Saul H. Rosenberg,[1] and Steven W. Elmore[1]

[1]Global Pharmaceutical Research and Development, Abbott Laboratories, Abbott Park, Illinois and [2]Idun Pharmaceuticals, San Diego, California

Abstract

Inhibition of the prosurvival members of the Bcl-2 family of proteins represents an attractive strategy for the treatment of cancer. We have previously reported the activity of ABT-737, a potent inhibitor of Bcl-2, Bcl-X_L, and Bcl-w, which exhibits monotherapy efficacy in xenograft models of small-cell lung cancer and lymphoma and potentiates the activity of numerous cytotoxic agents. Here we describe the biological activity of A-385358, a small molecule with relative selectivity for binding to Bcl-X_L versus Bcl-2 (K_i's of 0.80 and 67 nmol/L for Bcl-X_L and Bcl-2, respectively). This compound efficiently enters cells and co-localizes with the mitochondrial membrane. Although A-385358 shows relatively modest single-agent cytotoxic activity against most tumor cell lines, it has an EC_{50} of <500 nmol/L in cells dependent on Bcl-X_L for survival. In addition, A-385358 enhances the *in vitro* cytotoxic activity of numerous chemotherapeutic agents (paclitaxel, etoposide, cisplatin, and doxorubicin) in several tumor cell lines. In A549 non–small-cell lung cancer cells, A-385358 potentiates the activity of paclitaxel by as much as 25-fold. Importantly, A-385358 also potentiated the activity of paclitaxel *in vivo*. Significant inhibition of tumor growth was observed when A-385358 was added to maximally tolerated or half maximally tolerated doses of paclitaxel in the A549 xenograft model. In tumors, the combination therapy also resulted in a significant increase in mitotic arrest followed by apoptosis relative to paclitaxel monotherapy. (Cancer Res 2006; 66(17): 8731-9)

Introduction

Defects in the ability to appropriately regulate apoptotic processes are one of the fundamental occurrences that underlie cancer (1). Tumor initiation, progression to metastatic disease, and resistance to chemotherapeutic intervention all have been linked to apoptotic dysregulation (2–7). The central mediators of apoptosis are the Bcl-2 family of proteins that are composed of multiple prosurvival (Bcl-2, Bcl-X_L, Bcl-w, Mcl-1, and A1) as well as proapoptotic (Bax, Bak, Bad, Bid, Bim, Noxa, etc.) members (8). These proteins control apoptosis through a complex panoply of protein-protein interactions between the prosurvival members and a subset of the BH3-only proapoptotic class (e.g., Bim and Noxa; refs. 8–11). This, in turn, facilitates the function of the second class of proapoptotic proteins, Bax and Bak, resulting in the induction of a network of proteins (e.g., caspases) that execute cellular destruction (9, 10).

The elucidation of the three-dimensional structures of several Bcl-2 family members, as well as an improved understanding of the roles of the protein-protein interactions in regulating apoptosis, has suggested opportunities for developing chemotherapeutic agents that interfere with the prosurvival components of this process (12–19). Strategies currently under investigation include inhibition of protein expression as well as disruption of protein-protein interactions by the use of modified peptides, natural product analogues, and small organic molecules (20–27). An important unresolved question is whether inhibition of one or multiple prosurvival proteins will provide the optimal therapeutic advantage. The importance of Bcl-2 in neoplastic diseases is well established owing to the overexpression of this protein in multiple tumor types as well as the identification of the t(14;18) translocation as an initiating event in non-Hodgkin's lymphoma (4, 28). The importance of Bcl-X_L as a target is suggested by the fact that this protein is overexpressed in numerous tumor types and is associated with the development of disease progression (5, 29). In addition, Bcl-X_L expression is strongly correlated with resistance to a large variety of chemotherapeutic agents, suggesting that inhibition of this protein could be especially important as a potentiator of chemo-efficacy (30–32).

Previously, we have reported the biological activity of ABT-737, a potent inhibitor of Bcl-2, Bcl-X_L, and Bcl-w (27). This broad-spectrum Bcl-2 family inhibitor elicits robust single-agent activity in xenograft models, in addition to potentiating the activity of numerous cytotoxic agents. Here, we describe the activity of A-385358, a compound with relative selectivity for inhibition Bcl-X_L. Although this compound does not show single-agent activity *in vivo*, it was found to effectively potentiate the activity of numerous cytotoxic agents in a variety of cancer cells. In addition, the combination of A-385358 plus paclitaxel resulted in improved *in vivo* efficacy relative to paclitaxel monotherapy.

Note: Supplementary data for this article are available at Cancer Research Online (http://cancerres.aacrjournals.org/).

Requests for reprints: Alex R. Shoemaker, Global Pharmaceutical Research and Development, Abbott Laboratories, Abbott Park, IL 60064. Phone: 847-935-0869; Fax: 847-938-3266; E-mail: alex.shoemaker@abbott.com.

doi:10.1158/0008-5472.CAN-06-0367

Materials and Methods

A-385358

A-385358 [(*R*)-4-(3-dimethylamino-1-phenylsulfanylmethyl-propylamino)-*N*-[4-(4,4-dimethyl-piperidin-1-yl)-benzoyl]-3-nitro-benzenesulfonamide; MW = 639.83] was synthesized as described (33).

Affinity for Bcl-2 Family Members

The affinity of A-385358 (and its enantiomer) for Bcl-X_L and Bcl-2 was measured with a fluorescence polarization assay (34). The constructs used for Bcl-2 and Bcl-X_L as well as the labeled probes used in the competition assays were previously described (27, 34).

Cellular Uptake and Localization

Cellular uptake. FL5.12 cells suspended in EMB growth medium containing 4% fetal bovine serum (FBS) were incubated at 37°C for 1 hour in 10 μmol/L A-385358. Compound concentration was determined by high-performance liquid chromatography before and after the 1-hour incubation following brief centrifugation. To analyze membrane-bound fractions following compound incubation, cells were washed once with 10 volumes of cold PBS and lysed with 4 mL of water. A-385358 concentration was determined from aliquots of lysate before and after centrifugation.

Cellular localization. NCI-H460 lung carcinoma cells grown on glass coverslips were stained first with 20 nmol/L MitoTracker Green FM ($Ex_{490\ nm}$/$Em_{516\ nm}$), a mitochondria-specific fluorescent dye, for 15 minutes. The cells were washed once with PBS and incubated with fresh medium containing 50 μmol/L of compound 1 (6-{2-[4-(4,4-difluoro-5-thiophen-2-yl-3a,4a-diaza-4-bora-s-indacen-3-yl)-phenoxy]-acetylamino}-hexanoic acid (5*R*-{4-[4-(4,4-dimethyl-piperidin-1-yl)-benzoylsulfamoyl]-2-nitro-phenylamino}-6-phenylsulfanyl-hexyl)-amide), a close structural analogue of A-385358 conjugated to the fluorescent probe BODIPY Texas red-X, succinimidyl ester ($Ex_{588\ nm}$/$Em_{616\ nm}$). Approximately 30 minutes after the addition of the drug, live (unfixed) cells were imaged by confocal microscopy.

Paclitaxel uptake and efflux kinetics. A549 cells (1×10^5) were plated in 96-well plates in medium containing 10% fetal bovine serum. Following attachment, A-385358 was added to one set of wells (final concentration of 50 μmol/L in 10% FBS) and medium was added to another set. [^{3}H]Paclitaxel (5 μmol/L; 0.5 μCi/mL final concentration) was added to all wells and the cells were incubated at 37°C for various periods of time. For washout experiments, cells were exposed first to [^{3}H]paclitaxel for 2 hours. The cells were washed once with medium and then incubated with fresh medium with or without 50 μmol/L A-385358 at 37°C for various periods of time.

In vitro Activity

All tumor cell lines were obtained from the American Type Culture Collection (Menassas, VA) and cultured according to their recommendations. Cell viability was analyzed with the colorimetric 3-(4,5-dimethylthiazol-2-yl)-5-(3-carboxymethoxyphenyl)-2-(4-sulfophenyl)-2*H*-tetrazolium (MTS) assay (Promega Corp., Madison, WI) according to the instructions of the manufacturer. Cells were plated in 96-well plates at 5,000 per well 24 hours before treating with compound. For the UV-C assay, A549 cells were plated at 5,000 per well in 96-well plates. The following day, various doses of UV-C irradiation were applied using a Stratlinker (Stratagene, La Jolla, CA), immediately followed by addition of compound.

FL5.12 cells were propagated in RPMI 1640 supplemented with 10% FCS and 10% WEHI 3B conditional medium. Cells were stably transfected with either the *Bcl-xL* or *Bcl-2* gene under the regulation of the spleen focus-forming virus promoter. To determine compound-specific killing, transfected cells were cultured in the absence of WEHI 3B medium for 24 hours. Cells were then plated at 1×10^5 per well and serial dilutions of compound were added. Cell viability was measured by MTS assay after 24 hours of incubation. For Western blot analysis, 20 μg of total protein were electrophoresed on 4% to 12% Bis/Tris gradient gels (Invitrogen, Carlsbad, CA) and transferred to polyvinylidene difluoride membrane (Micron Separations, Inc., Westborough, MA). Specific signals were detected with primary antibodies to Bcl-X_L (Santa Cruz Biotechnology, Santa Cruz, CA) or Bcl-2 (Transduction Laboratories, La Jolla, CA).

In vivo Efficacy

All animal studies were conducted in accordance with the guidelines established by the internal Institutional Animal Care and Use Committee. For A549 xenograft studies, 5×10^6 cells were mixed with 50% Matrigel (BD Biosciences, Bedford, MA) and inoculated by s.c. injection into the flank of male severe combined immunodeficient (scid) mice (Charles River Laboratories, Wilmington, MA). For early-treatment studies, mice were randomly assigned to treatment groups and therapy was initiated on day 7 following inoculation. For established tumor studies, tumors were allowed to grow to the indicated size and then assigned to therapy groups. Tumor growth was analyzed by measurement with digital calipers and tumor volume was estimated from the formula $(L \times W^2)/2$. Effects on tumor growth rate were assessed by determining %T/C [(mean tumor volume of treated group on day x / mean tumor volume of control group on day x) × 100]. Effects on tumor growth delay were assessed by determining percent increase in life span (%ILS) as measured by the time for tumors to reach a predetermined end point [%ILS = (median time for tumors in treated group to reach size x / median time for tumors in control group to reach size x) × 100]. LX-1 tumors were established from an *in vivo* propagated line. For efficacy studies, male CD-1 nude mice were inoculated with a 1:5 dilution of tumor brei in 50% Matrigel and analysis was conducted as described above. NCI-H146 xenograft studies were conducted as described (27). A-385358 was delivered in a vehicle containing 5% Tween 80, 20% propylene glycol, and 75% PBS (pH 3.8). Paclitaxel (Bristol-Myers Squibb, Co., Princeton, NJ) was formulated according to the recommendations of the manufacturer. For combination therapy of paclitaxel plus A-385358, both drugs were administered i.p. with the paclitaxel given several hours before treatment with A-385358 (except for immunohistochemistry studies looking at expression of MPM-2 and caspase-3 wherein the two drugs were given simultaneously).

Immunohistochemical Studies

Following the indicated drug treatments, A549 tumors were collected into Streck Tissue Fixative (Streck Laboratories, Inc., Omaha, NE) for 24 hours, processed, embedded in paraffin, and sectioned. For analysis of G_2-M arrest, the MPM-2 antibody (DAKO Corp., Carpinteria, CA), which recognizes a subset of microtubule phosphoproteins, was used at 1:350. For analysis of apoptosis, an antibody directed against the activated form of caspase-3 (BD PharMingen, San Diego, CA) was used at 1:400. Secondary antibodies were used at 1:250 followed by treatment with the StreptABC kit (DAKO) and 3,3′-diaminobenzidine (Sigma Chemical Co., St. Louis, MO). Quantitative analysis was conducted by analyzing the areas of highest density specific staining for each sample. Two to three samples were examined for each group and the number of positive cells per given area was scored at ×100 to ×200 magnification.

Results

Affinity of A-385358 for Bcl-X_L and Bcl-2. The binding affinities of A-385358 for Bcl-X_L and Bcl-2 were determined with fluorescence polarization assays, which measure the ability to displace fluorescein-labeled BH3 peptides. Under serum-free conditions, the K_i's of A-385358 for Bcl-X_L and Bcl-2 were 0.8 ± 0.17 ($n = 5$) and 67 ± 7 ($n = 6$) nmol/L, respectively. For Bcl-X_L, this binding is comparable to the Bad BH3 peptide (1.2 nmol/L), whereas for Bcl-2 the affinity is ~7-fold less than that of the peptide (9.1 nmol/L). The enantiomer, which bears the opposite configuration of the dimethylamino ethyl group, was 20- and 300-fold less active against Bcl-X_L and Bcl-2, respectively, and was used as a negative control in cellular assays. In contrast, the affinity of ABT-737 for both Bcl-X_L and Bcl-2 was well below the detection limit of 0.5 and 1 nmol/L, respectively (27).

Cellular uptake and localization of A-385358. To show that A-385358 effectively enters cells and associates with the appropriate cellular target, uptake and co-localization studies were conducted in FL5.12 and NIH-H460 cells, respectively.

A-385358 was added to a preparation of FL5.12 cells at a concentration of 10 μmol/L and the cells were incubated at 37°C for 1 hour. Following centrifugation, drug concentration was determined in both the cellular and extracellular fractions by high-performance liquid chromatography analysis. The [cell]/[extracellular] ratio of 51.1 ± 2.7 indicates significant association of A-385358 with cells. To determine the distribution of A-385358 within cells, purified cellular preparations were lysed and centrifuged with compound concentration determined in the pellet and supernatant fractions. Thirty percent of the compound associated with cells was released on lysis, indicating that the majority of A-385358 was bound to cellular membranes.

To evaluate intracellular localization, a fluorescent probe (compound 1) was prepared from a structurally similar analogue to A-385358, which could be visualized by confocal microscopy. H460 cells were first stained with the mitochondrial marker MitoTracker Green FM and then treated with 50 μmol/L compound 1 before confocal imaging of the unfixed cells. Analysis of the merged image shows that compound 1 colocalizes with MitoTracker Green at the mitochondria (Fig. 1).

A-385358 restores interleukin-3 dependency to FL5.12/Bcl-X_L cells. FL5.12 is a murine pro-B lymphocytic cell line that is dependent on interleukin-3 (IL-3) for survival (35). However, overexpression of anti-apoptotic proteins such as Bcl-X_L and Bcl-2 can protect against apoptosis that accompanies cytokine withdrawal in this cell line (31). Treatment of IL-3-deprived FL5.12/Bcl-X_L cells for 24 hours with A-385358 resulted in cell killing with an EC_{50} of 0.47 ± 0.05 μmol/L (n = 68). This effect was accompanied by an increase in caspase-3 activity (data not shown). Consistent with the greater affinity for the Bcl-X_L versus Bcl-2 hydrophobic grooves, the EC_{50} of A-385358 for IL-3-depleted FL5.12/Bcl-2 cells (1.9 ± 0.1 μmol/L; n = 55) was 4-fold higher relative to the cytokine-deprived FL5.12/Bcl-X_L cells. In addition, A-385358 was more effective at stimulating cytochrome c release from mitochondria isolated from FL5.12/Bcl-X_L versus Bcl-2 cells (data not shown). The EC_{50} of the enantiomer was ~10 μmol/L in both cell lines. These data suggest that low nanomolar binding affinity to the requisite Bcl-2 family member may be needed for efficient killing of these cells, and this is consistent with the observation that ABT-737 exhibited highly potent killing of both IL-3-deprived FL5.12/Bcl-X_L and FL5.12/Bcl-2 cells (0.03 ± 0.01 and 0.007 ± 0.001 μmol/L, respectively).

A-385358 enhances the activity of cytotoxic agents in cancer cells *in vitro*. We have previously reported that ABT-737 exhibits potent cell killing of small-cell lung cancer and lymphoid cells but displays rather weak single-agent activity against most other tumor cell lines. This *in vitro* potency translated into robust *in vivo* single-agent activity, particularly in xenograft models of small-cell lung cancer wherein complete regression of established tumors was observed (27). Like ABT-737, A-385358 was most active against small-cell lung cancer and leukemia cells, although A-385358 was significantly less potent than ABT-737 (Table 1). The EC_{50} for A-385358 was ~20-fold lower than that of ABT-737 in H146 cells under serum-free conditions and A-385358 also exhibited a greater loss of potency in the presence of 10% serum (Table 1). The monotherapy activity of A-385358 was also examined in the H146 xenograft small-cell lung cancer model. When administered at 100 mg/kg/d, i.p., for 21 days, only modest inhibition of tumor growth was observed (Table 1). In contrast, ABT-737 at equivalent plasma exposure significantly inhibited tumor growth, including complete regression of a majority of tumors (Table 1; ref. 27).

Although A-385358 did not show significant single-agent activity, we sought to determine whether it inhibited Bcl-2 family proteins sufficiently to potentiate the effect of other chemotherapies (as measured by shifting the EC_{50} and/or enhancing the extent of cell killing). Human tumor cell lines were incubated for 48 hours with varying concentrations of cytotoxic agents with or without A-385358 at concentrations ranging from 2.5 to 10.0 μmol/L. The cellular EC_{50} was determined by MTS assay. A-385358 was able to enhance by a factor of 2 or more the cell killing activity of paclitaxel and doxorubicin in A549 cells, of etoposide in A549, SN12C, and 786-O cells, and of cisplatin in SN12C, MiaPaCa-2, NCI-H226, and NCI-H322M cells (Table 2; Fig. 2). Interestingly, the ability of A-385358 to enhance chemotherapeutic cytotoxicity seemed to be schedule dependent. When coincubated for 48 hours, A-385358 potentiated (i.e., shifted the EC_{50}) the activity of paclitaxel in A549 cells by a factor of 3.5. Under these same conditions, ABT-737 shifted the EC_{50} of paclitaxel by 4-fold in A549 cells (27). However, when paclitaxel was given 24 hours before addition of 10 μmol/L A-385358 with a subsequent 48 or 72 hours of co-incubation, the potentiation factor was increased to 15- and 26-fold, respectively (Fig. 2). The enantiomer did not potentiate the activity of paclitaxel at concentrations as high as 20 μmol/L (data not shown). One possible explanation for these results was that A-385358 might have indirectly enhanced cell killing due to increased uptake or reduced efflux of the cytotoxic drug. To address this possibility, A549 cells were incubated with [^{3}H]paclitaxel in the presence or absence of 50 μmol/L A-385358.

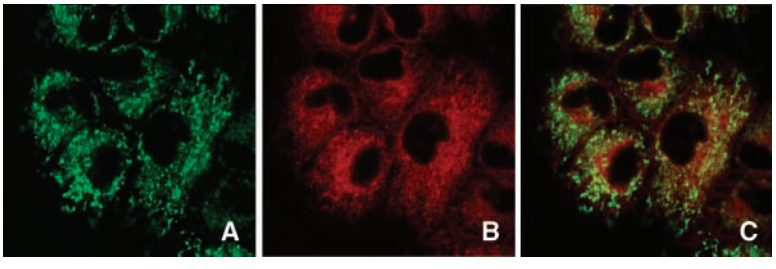

Figure 1. Compound 1 co-localizes with mitochondria in NCI-H460 cells. NCI-H460 cells were costained with MitoTracker Green FM and compound 1 (a close structural analogue of A-385358 labeled with BODIPY Texas red-X) and imaged by confocal microscopy. *A,* localization of MitoTracker Green FM. *B,* localization of compound 1. *C,* merged image of the two stains.

Table 1. Potency of A-385358 and ABT-737 in human tumor cell lines

Cell line	Compound			
	A-385358	A-385358-e*	ABT-737	ABT-737-e†
H146				
Serum-free	0.35 ± 0.03 (2)	6.1 ± 0.1 (2)	0.015 ± 0.006 (5)	0.43 ± 0.12 (4)
10% HS‡	31 ± 6 (5)	62.3 (1)	0.09 ± 0.04 (18)	12 ± 5 (6)
%TGI *in vivo*§	29	ND	92	ND
Molt-4				
Serum-free	0.74 ± 0.23 (3)	5.5 ± 1.3 (3)	0.004 ± 0.002 (3)	0.46 ± 0.03 (3)
10% HS	32.8 ± 10.3 (2)	>50 (2)	0.71 ± 0.44 (7)	22.2 ± 3.2 (3)
CCRF-CEM				
Serum-free	0.21 ± 0.12 (4)	2.7 ± 0.5 (4)	0.002 (1)	0.87 (1)
10% HS	>30 (2)	>50 (2)	0.3 ± 0.1 (4)	17 ± 6 (3)
A549				
Serum-free	16 ± 1 (2)	>20 (2)	5.2 ± 0.2 (2)	12 ± 0 (2)
10% HS	>100 (4)	>100 (4)	22.3 ± 5.0 (3)	>100 (3)

NOTE: Data are given as mean EC_{50} (μmol/L) ± SE (*n*).
*The enantiomer for A-385358.
†The enantiomer for ABT-737.
‡Cells grown in 10% human serum.
§Percent tumor growth inhibition. H146 tumors were size matched at ~225 mm^3 in scid mice and A-385358 or ABT-737 was administered at 100 mg/kg/d, i.p., for 21 days. %TGI reported using tumor measurements at the end of the dosing period.

As shown in Figure 2*C*, the kinetics and extent of paclitaxel uptake and release were not altered by the presence of A-385358.

To more explicitly rule out drug-drug interactions as a cause for the observed chemopotentiation, A-385358 was also examined in combination with UV radiation. A549 cells were exposed to different doses of UV-C irradiation followed by 48-hour incubation with A-385358 at various concentrations. As was observed with the chemotherapeutic drug combinations, A-385358 enhanced cell killing by UV-C by ~2-fold (Table 2). Treatment of A549 cells with the enantiomer produced no enhancement of UV-C–mediated cell killing at concentrations up to 20 μmol/L (data not shown). In addition, A-385358 treatment increased the extent of kill induced by UV irradiation. The percentage of viable A549 cells was not significantly different at the two highest doses of UV-C tested (35 ± 6% at 16 mJ/cm^2 versus 29 ± 3% at 32 mJ/cm^2). However, in the presence of 1.25 μmol/L A-385358, the fraction of viable cells

Table 2. A-385358 enhances cell killing of various cytotoxic agents in human tumor cell lines

Cell line	Tumor type	Chemotherapeutic	A-385358 (μmol/L)*	Potentiation factor†
A549	NSCL	Etoposide	10	13 ± 1 (2)
		Doxorubicin	10	3.6 ± 0.7 (5)
SN12C	Renal	Cisplatin	5	3.3 ± 0.1 (2)
		Etoposide	5	2.3 ± 0.1 (2)
		UV-C	2.5	2.1 ± 0.3 (2)
786-O	Renal	Etoposide	2.5	2.3 ± 0.1 (2)
MiaPaCa	Pancreas	Cisplatin	5‡	2.6 (1)
NCI-H226	NSCL	Cisplatin	2.5	2.4 ± 0.7 (2)
		Doxorubicin	2.5	1.8 ± 0.1 (2)
NCI-H322M	NSCL	Cisplatin	10	2.0 ± 0 (2)
DLD-1	Colon	Cisplatin	10‡	1.8 (1)
A549	NSCL	UV-C	2.5	1.5 ± 0.1
A549	NSCL	UV-C	5	1.8 ± 0.2
A549	NSCL	UV-C	10	2.2 ± 0.2

*Serum-free conditions unless otherwise specified; 48-hour co-treatment.
†Ratio of EC_{50} for chemotherapeutic alone to EC_{50} of chemotherapeutic in combination with A-385358; mean ± SE (*n*).
‡3% FBS.

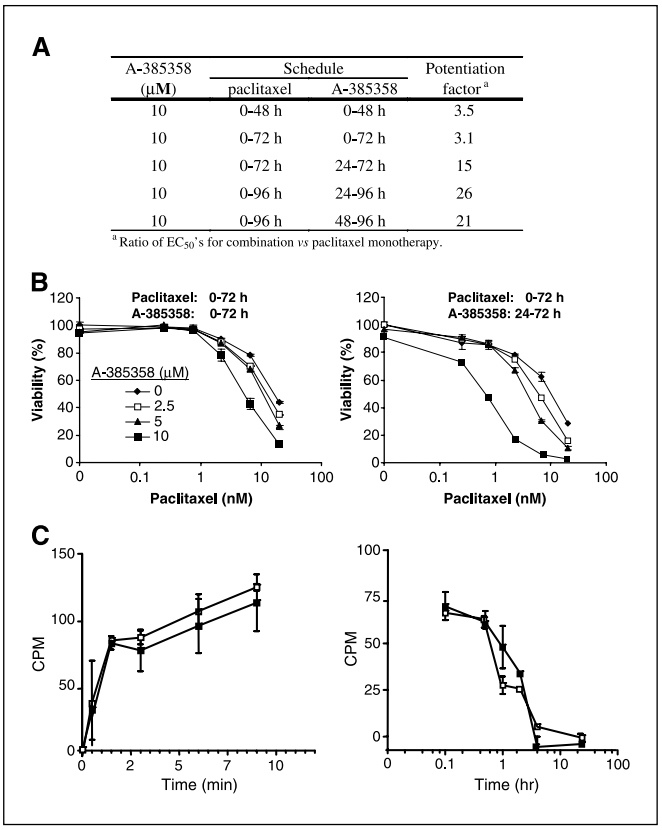

Figure 2. Analysis of A-385358 in combination with paclitaxel in A549 non–small-cell lung cancer cells. *A,* schedule dependency of cell killing in A549 cells grown in serum-free medium. Paclitaxel was given either before or concurrently with A-385358 and the potentiation factor was determined by examining the EC_{50} ratio for the combination versus paclitaxel monotherapy. *B,* dose-response curves for paclitaxel plus A-385358 given concurrently for 72 hours or with A-385358 given 24 hours after treatment with paclitaxel. *C,* A-385358 has no effect on the uptake or release of paclitaxel from A549 cells. A549 cells were cultured with [^{3}H]paclitaxel in the presence or absence of 50 μmol/L A-385358 and the association (*left*) or dissociation (*right*) of radioactivity with the cells was measured over time. ■, medium only; □, 50 μmol/L A-385358 added.

observed after 16 mJ/cm^2 of UV-C was reduced to <10%. Thus, A-385358 was able to reduce the EC_{90} by at least a factor of 2. Similar enhancement in the extent of cell kill was observed with ABT-737 plus UV-C and A-385358 plus paclitaxel in A549 cells (Fig. 2*B*, data not shown, and ref. 27).

A-385358 enhances the efficacy of paclitaxel *in vivo*. A series of experiments were conducted to evaluate the ability of A-385358 to potentiate cytotoxic activity *in vivo*. Initial studies were conducted using an early-treatment A549 non–small-cell lung cancer xenograft model in which therapy was initiated 7 days after inoculation (before the development of measurable tumors). A-385358 given once daily at 100 mg/kg/d, i.p., from day 7 to 27 was well tolerated (<5% body weight loss) and provided no significant inhibition of tumor growth (Fig. 3*A*). When paclitaxel was given i.p. at 15 or 30 mg/kg/d (the maximum tolerated dose) on a q4d ×3 schedule, a 45% to 50% inhibition of tumor growth was observed (Supplementary Table S1). When given in combination, A-385358 significantly enhanced the activity of paclitaxel given at either of these doses (Fig. 3*A*; Supplementary Table S1). The combination of A-385358 given at 100 mg/kg/d plus the lower dose of paclitaxel produced a significant reduction in tumor growth (%T/C) compared with paclitaxel monotherapy (Supplementary Table S1). This combination also yielded a >100% increase in time for tumors to reach 900 mm^3 (%ILS) compared with vehicle control (Supplementary Table S1). Maximal efficacy was observed during the dosing period for A-385358, with slow but steady increase in the tumor growth after termination of treatment. The combination of A-385358 at 75 mg/kg/d plus paclitaxel at 30 mg/kg/d was also well tolerated and inhibited tumor growth rate by nearly 80% (Supplementary Table S1). Significant effects on tumor growth relative to paclitaxel monotherapy were observed with doses as low as 50 mg/kg/d (data not shown).

As a more rigorous test of the ability of A-385358 to potentiate the efficacy of paclitaxel, a staged A549 xenograft model was used. In these experiments, tumors were allowed to grow to ~240 mm^3 (day 15 post-inoculation) before assignment to treatment groups and initiation of therapy. In this setting, the combination of A-385358 at 100 mg/kg/d plus paclitaxel at 15 mg/kg/d resulted in nearly complete inhibition of tumor growth during the majority of the A-385358 therapy period (Fig. 3*C*). After termination of therapy, the tumor growth rate increased and paralleled that observed for the paclitaxel monotherapy group. The efficacy observed with this combination was quite comparable to that observed for paclitaxel given at the maximum tolerated dose. In contrast, the combination of paclitaxel at 30 mg/kg/d plus A-385358 at 75 mg/kg/d led to regression of these established tumors (Fig. 3*D*). In the period following the last dose of paclitaxel, the average tumor size was reduced to ~200 mm^3 from an initial peak of 400 mm^3. Tumor growth then slowly increased to eventually parallel that observed for paclitaxel monotherapy. The enhanced inhibition of tumor growth as measured by ratios of tumor size (%T/C = 25) and tumor growth delay (%ILS = 180) were both highly significant compared with the effects observed with the maximum tolerated dose of paclitaxel given alone.

To interpret the significance of combination therapy *in vivo*, it is important to consider potential drug-drug interactions that could have affected the pharmacokinetic properties of the cytotoxic agent. Co-administration of A-385358 plus paclitaxel did not alter either the C_{max} (3.0 μg/mL) or the AUC (13 μg h/mL) of paclitaxel relative to dosing with paclitaxel alone in scid mice (33). Thus, the improved efficacy observed with the combination of A-385358 plus paclitaxel was not the result of A-385358-mediated enhancement of paclitaxel exposure.

The combination of A-385358 plus paclitaxel was also evaluated in the LX-1 squamous cell lung carcinoma model. Owing to the relatively high sensitivity of LX-1 tumors to paclitaxel therapy, A-385358 (at 100 mg/kg/d) was given in combination with paclitaxel at 5 mg/kg/d. Although the effect was less robust than that observed in the A549 model, A-385358 improved significantly the efficacy of monotherapy in LX-1-treated tumors (Fig. 3*B*). The 65% inhibition of tumor growth rate and 30% enhancement of tumor growth delay were both statistically significant relative to the results obtained for paclitaxel monotherapy.

Previous work has shown that paclitaxel treatment of xenograft tumors results in a characteristic mitotic arrest followed by apoptosis. In breast and ovarian tumors, the peak mitotic arrest and apoptosis occur ~8 to 10 and 18 to 24 hours after a single dose of paclitaxel, respectively (36). To examine the *in vivo* cellular response to A-385358, established A549 tumor–bearing animals were treated with a single dose of A-385358, paclitaxel, or both, and tumors were harvested at various times after treatment (Fig. 4).

To analyze mitotic arrest, immunohistochemistry was done using an MPM-2 antibody that recognizes several phosphoproteins expressed specifically during mitosis (37). The apoptotic response was analyzed with an antibody specific for the activated form of caspase-3. For paclitaxel given alone, peak mitotic arrest was observed ~24 to 30 hours after treatment (Fig. 4*B*). When A-385358 was given in combination with paclitaxel, the timing of arrest was similar to that observed with paclitaxel monotherapy; however, the percentage of MPM-2-positive cells was increased by ~2-fold. Analysis of caspase-3 expression showed that the peak apoptotic index following paclitaxel treatment occurred at 30 hours (Fig. 4*C*). However, addition of A-385358 seemed to extend the apoptotic response. Whereas the apoptotic response had returned to basal levels by 36 hours after treatment with paclitaxel, significant numbers of caspase-3-positive cells were still observed at 36 hours in the combination treatment group (Fig. 4*C*).

Discussion

Although dysregulation of the Bcl-2 family of apoptosis regulators has long been implicated in the genesis and progression of cancer, the specific functions of these genes in this disease process remain poorly understood. Numerous studies have reported the overexpression of Bcl-2 in lymphoma, lung, and colon cancer (28, 38, 39). Furthermore, increased Bcl-2 expression is associated with disease progression including the emergence of metastatic disease and the development of hormone refractory breast and prostate cancer (40, 41). Both Bcl-2 and Bcl-X_L are also implicated strongly in chemoresistance involving multiple classes of cytotoxic agents in numerous tumor types (2, 42, 43). Indeed, Amundson et al. (30) showed that Bcl-X_L expression correlates with resistance to more than 100 standard chemotherapy agents. This correlation was p53 independent and was of higher statistical significance than the correlation with *p53* mutational status.

It has now been established with ABT-737 that broad-spectrum Bcl-2 family inhibitors can elicit significant single-agent activity, both *in vitro* and *in vivo*, in addition to potentiating the activity of chemotherapeutic agents (27). The present study was undertaken to evaluate the biological activity of a compound with a more Bcl-X_L-specific selectivity profile. The results presented here with A-385358 show that a compound with potent affinity for Bcl-X_L is indeed sufficient to enhance the activity of a variety of chemotherapeutic agents in diverse cancer cell lines.

To show mechanism-based activity in cells, A-385358 was shown to co-localize to the mitochondrial membrane and to reverse Bcl-X_L-mediated protection of FL5.12 cells from cytokine withdrawal (Fig. 1). Although A-385358 and ABT-737 exhibit similar patterns of sensitivity across a diverse panel of tumor cell lines, ABT-737 is

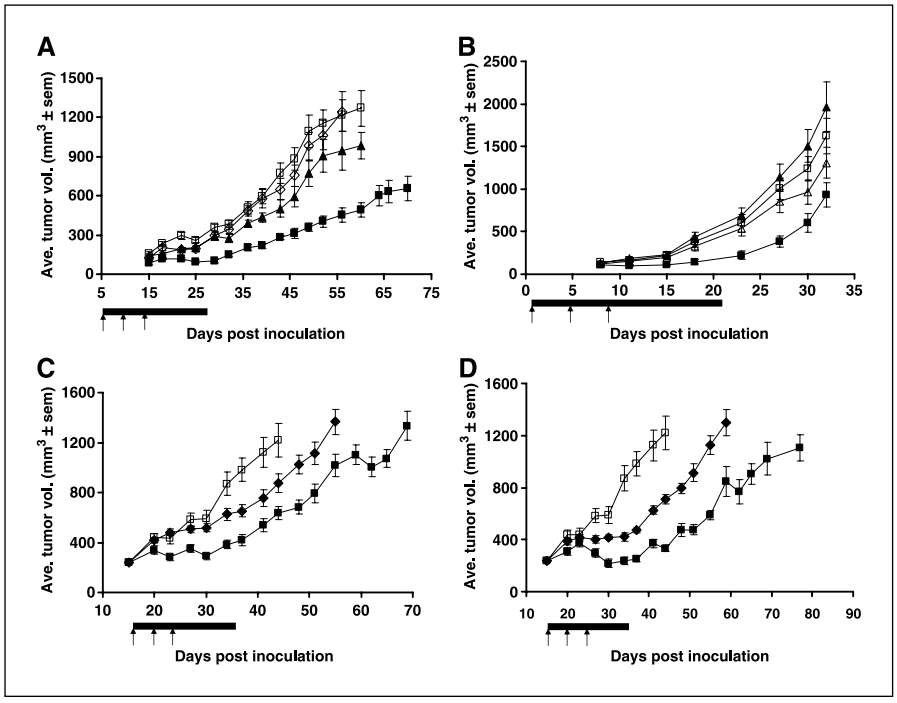

Figure 3. Effect of A-385358 in combination with paclitaxel in xenograft models. *A,* A-385358 plus paclitaxel in the early-treatment A549 model. Mice (n = 10 per group) were randomly assigned to treatment groups following inoculation and therapy was initiated on day 7. A-385358 (◇) was administered i.p. once daily at 100 mg/kg/d on days 7-27 (*black bar*). Paclitaxel (▲) was given at 15 mg/kg/d, i.p., on days 7, 11, and 15 (*arrows*). The combination therapy (■) led to a significantly reduced tumor growth rate (%T/C; $P < 0.0001$) and enhanced tumor growth delay (%ILS; $P < 0.01$) compared with paclitaxel monotherapy. □, mice treated with the combination vehicles. *B,* A-385358 plus paclitaxel in the early-treatment LX-1 lung cancer model. Mice were randomly assigned to treatment groups following inoculation and therapy was initiated on day 1. A-385358 (△) was administered once daily at 100 mg/kg/d on days 1-21 (*black bar*). Paclitaxel (□) was given at 5 mg/kg/d, i.p., on days 1, 5, and 9 (*arrows*). The combination therapy (■) led to a significantly reduced tumor growth rate (%T/C; $P < 0.002$) and enhanced tumor growth delay (%ILS; $P < 0.02$) compared with monotherapy. ▲, mice treated with the combination vehicle. Data combined from two independent efficacy trials (N = 20 mice per group). *C* and *D,* effect of A-385358 in combination with paclitaxel in the staged tumor A549 xenograft model. Fifteen days after inoculation, mice were assigned to treatment groups (N = 10 mice per group) with an average tumor size of 240 mm^3 per group. *C,* A-385358 was administered i.p. once daily at 100 mg/kg/d on days 16 to 36 (*black bar*). Paclitaxel (♦) was given at 15 mg/kg/d, i.p., on days 16, 20, and 24 (*arrows*). The combination therapy (■) led to a significantly reduced tumor growth rate (%T/C; $P < 0.01$) and enhanced tumor growth delay (%ILS; $P < 0.01$) compared with paclitaxel monotherapy. □, mice treated with the combination vehicle. *D,* A-385358 was administered i.p. once daily at 75 mg/kg/d on days 16 to 36 (*black bar*). Paclitaxel (♦) was given at the maximum tolerated dose of 30 mg/kg/d, i.p., on days 16, 20, and 24 (*arrows*). The combination therapy (■) led to a significantly reduced tumor growth rate (%T/C; $P < 0.001$) and enhanced tumor growth delay (%ILS; $P < 0.02$) compared with paclitaxel monotherapy. □, mice treated with the combination vehicle.

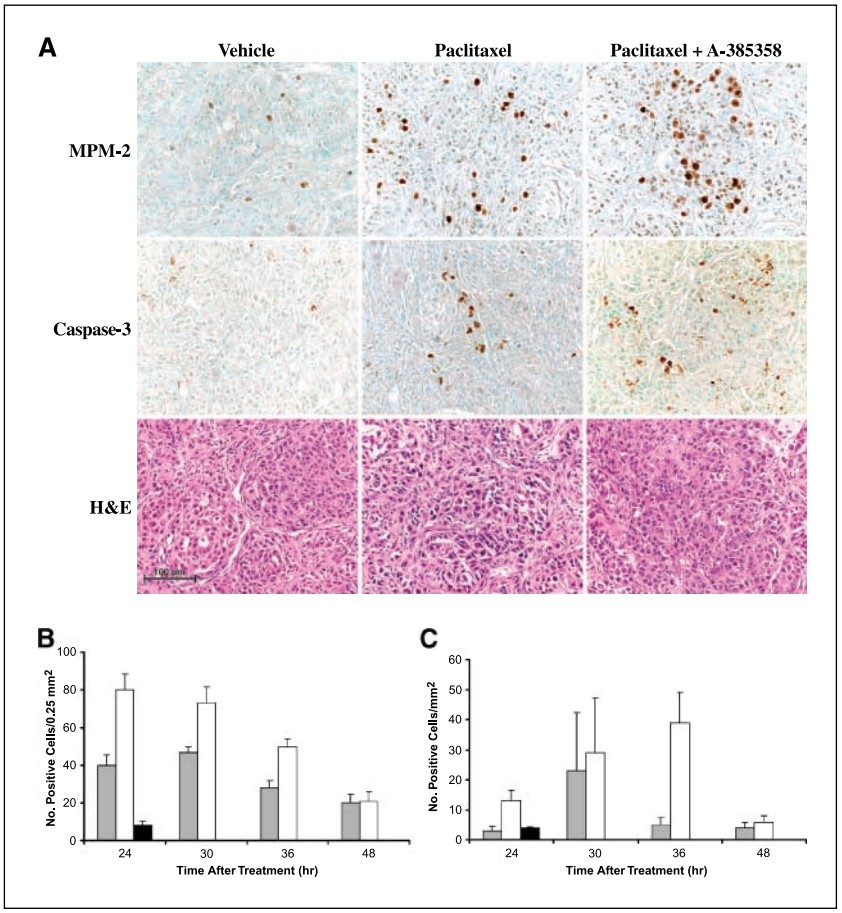

Figure 4. Immunohistochemical analysis of MPM-2 and caspase-3 expression in A549 tumors. scid mice bearing established A549 tumors were treated with vehicle, paclitaxel, or paclitaxel plus A-385358. *A,* mice were given a single dose of paclitaxel at 15 mg/kg and/or A-385358 at 100 mg/kg or the combination vehicle and tumors were harvested 30 hours later (vehicles were harvested 1 hour after treatment). *B* and *C,* quantitative analysis of MPM-2 (*B*) and caspase-3 (*C*) immunohistochemistry in A549 tumors. Mice bearing established A549 tumors were treated as in (*A*). Quantitative analysis was done by counting positive cells from two to three samples from each group at ×200 to ×300 magnification. *Gray bars,* paclitaxel; *open bars,* combination; *black bars,* vehicle.

significantly more potent than A-385358 in all cell lines tested (Table 1; ref. 27). Furthermore, ABT-737 monotherapy of small-cell lung cancer xenografts resulted in highly significant inhibition of tumor growth whereas A-385358 had only modest single-agent activity (Table 1; ref. 27). As ABT-737 is a more potent inhibitor of both Bcl-2 and Bcl-X_L, it is possible that the stronger biological activity in human tumor cell lines associated with ABT-737 is attributable, at least in part, to the stronger affinity for Bcl-X_L.

The analysis of A-385358 plus cytotoxic agents *in vitro* showed an especially strong potentiation of paclitaxel in A549 cells (Fig. 2). This effect was most pronounced when cells were preincubated with paclitaxel before addition of the Bcl-X_L inhibitor. To determine whether this potentiation could translate to enhanced antitumor efficacy *in vivo*, a series of experiments were conducted in xenograft models (Fig. 3). These results indicate that A-385358 can indeed potentiate the efficacy of paclitaxel on both an early-treatment schedule as well as on established tumors. In the early-treatment model, complete inhibition of tumor growth was observed during treatment with A-385358, whereas in the staged model tumor regression was observed (Fig. 3). Interestingly, ABT-737 and A-385358 showed a similar extent of potentiation when coincubated with paclitaxel in A549 cells *in vitro*, although ABT-737 is a more potent inhibitor of both Bcl-2 and Bcl-X_L. ABT-737 also significantly enhances the *in vivo* efficacy of numerous cytototoxic agents in xenograft models, including antimitotic agents (27).

Although paclitaxel is efficacious in the A549 xenograft tumor model, this activity is rather weak relative to that observed in many other models. Furthermore, A549 tumors seem to be generally chemoresistant as they show little or no response to a variety of other chemotherapeutic agents, despite the fact that these cells express functional p53 (44). Although A549 cells express relatively low levels of Bcl-2, expression of Bcl-X_L is among the highest reported for the NCI-60 cell line panel, suggesting that Bcl-X_L may be a key component of drug resistance in this tumor (30, 45). There does not seem to be a direct correlation between absolute levels of Bcl-X_L expression and extent of potentiation of other cytotoxic agents. However, it will be important to characterize drug-induced changes in Bcl-X_L expression in each of the other tumor lines examined. A recent report has suggested that a key component of resistance to paclitaxel therapy in tumors with activated *RAS* (such as A549) may involve targeted degradation of the proapoptotic protein Bim (46). An additional link between the activity of paclitaxel and the function of Bcl-2 family members involves the finding that reduced activity of Bcl-2 and/or Bcl-X_L may result from paclitaxel-mediated phosphorylation of these proteins (47–50). Thus, the combination of paclitaxel and A-385358 may have cooperative effects on the inhibition of prosurvival Bcl-2 family proteins and the consequences of these effects may be especially profound in *RAS* mutant tumors such as A549. Efficacy in the *RAS* mutant LX-1 model showed that the ability of A-385358 to potentiate paclitaxel is not unique to A549 tumors. It will be of interest to determine if the correlation between *RAS* status and sensitivity to A-385358 extends beyond potentiation of paclitaxel. Preliminary studies have shown a significant but transient enhancement of gemcitabine activity by

A-385358 in the *RAS* mutant MiaPaCa-2 xenograft model (data not shown).

When studying the biological activity of two compounds given in combination, it is important to eliminate the possibility of contributions that are the result of drug-drug interactions. Through several lines of experimentation, we have shown that the activity of A-385358 is not the result of such indirect effects. First, the examination of [^{3}H]paclitaxel in A549 cells showed that A-385358 does not influence either the uptake or efflux of paclitaxel in these cells (Fig. 2*C*). Second, analysis of drug levels in mice showed that paclitaxel plasma concentration was not altered significantly by co-dosing with A-385358 (33). This result is important to rule out the possibility of metabolic interactions and/or inhibition of drug transporters. Finally, *in vitro* analysis of A-385358 in combination with UV-C irradiation showed potentiation similar to that observed in combination with various cytotoxic drugs (Table 2).

Immunohistochemical analysis of A549 tumors showed that A-385358 enhances the apoptotic activity of paclitaxel (Fig. 4). Milas et al. (36) showed that treatment with paclitaxel leads to significant apoptosis that is preceded by mitotic arrest. Addition of A-385358 seemed to extend the apoptotic response with significant caspase-3 activity observed from 24 to 36 hours after a single treatment with both paclitaxel and A-385358. Interestingly, although the timing of mitotic arrest (as observed with MPM-2 staining) was similar with cotreatment, the absolute level of MPM-2 staining was increased following treatment with A-385358 (Fig. 4). These results suggest that MPM-2 staining may detect cells in the transition from mitotic arrest to apoptosis or that alteration of proapoptotic Bcl-X_L/Bcl-2 function by treatment with A-385358 may in itself influence the onset and/or duration mitotic arrest following treatment with paclitaxel.

We have described here a small-molecule inhibitor of Bcl-X_L that potentiates the activity of cytotoxic agents both *in vitro* and *in vivo*. These results extend our previous findings reported with ABT-737 and show that potent inhibition of Bcl-X_L alone is sufficient to significantly potentiate the activity of chemotherapeutic agents both *in vitro* and *in vivo.* The future development of agents with varying selectivity profiles for inhibition of Bcl-2 family proteins will augment our understanding of the functions of these proteins in cancer development and progression and facilitate the development of effective proapoptotic cancer therapies.

Acknowledgments

Received 2/6/2006; revised 4/7/2006; accepted 6/2/2006.

The costs of publication of this article were defrayed in part by the payment of page charges. This article must therefore be hereby marked *advertisement* in accordance with 18 U.S.C. Section 1734 solely to indicate this fact.

References

1. Hanahan D, Weinberg RA. The hallmarks of cancer. Cell 2000;100:57–70.
2. Minn AJ, Rudin CM, Boise LH, Thompson CB. Expression of bcl-xL can confer a multidrug resistance phenotype. Blood 1995;86:1903–10.
3. Johnstone RW, Ruefli AA, Lowe SW. Apoptosis: a link between cancer genetics and chemotherapy. Cell 2002; 108:153–64.
4. Bakhshi A, Jensen JP, Goldman P, et al. Cloning the chromosomal breakpoint of t(14;18) human lymphomas: clustering around JH on chromosome 14 and near a transcriptional unit on 18. Cell 1985;41:899–906.
5. Espana L, Fernandez Y, Rubio N, Torregrosa A, Blanco J, Sierra A. Overexpression of Bcl-xL in human breast cancer cells enhances organ-selective lymph node metastasis. Breast Cancer Res Treat 2004;87:33–44.
6. Martin SS, Ridgeway AG, Pinkas J, et al. A cytoskeleton-based functional genetic screen identifies Bcl-xL as an enhancer of metastasis, but not primary tumor growth. Oncogene 2004;23:4641–5.
7. McDonnell TJ, Korsmeyer SJ. Progression from lymphoid hyperplasia to high-grade malignant lymphoma in mice transgenic for the t(14; 18). Nature 1991;349:254–6.
8. Cory S, Huang DC, Adams JM. The Bcl-2 family: roles in cell survival and oncogenesis. Oncogene 2003;22: 8590–607.
9. Jacobson MD, Burne JF, King MP, Miyashita T, Reed JC, Raff MC. Bcl-2 blocks apoptosis in cells lacking mitochondrial DNA. Nature 1993;361:365–9.
10. Wei MC, Zong WX, Cheng EHY, et al. Proapoptotic BAX and BAK: A requisite gateway to mitochondrial dysfunction and death. Science 2001;292:727–30.
11. Chen L, Willis SN, Wei A, et al. Differential targeting of prosurvival Bcl-2 proteins by their BH3-only ligands allows complementary apoptotic function. Mol Cell 2005;17:393–403.
12. Muchmore SW, Sattler M, Liang H, et al. X-ray and NMR structure of human bcl-xl, an inhibitor of programmed cell death. Nature 1996;381:335–41.
13. Petros AM, Medek A, Nettesheim DG, et al. Solution structure of the antiapoptotic protein bcl-2. Proc Natl Acad Sci U S A 2001;98:3012–7.
14. Petros AM, Olejniczak ET, Fesik SW. Structural biology of the Bcl-2 family of proteins. Biochim Biophys Acta 2004;1644:83–94.
15. Suzuki M, Youle RJ, Tjandra N. Structure of Bax: coregulation of dimer formation and intracellular localization. Cell 2000;103:645–54.
16. Denisov AY, Madiraju MS, Chen G, et al. Solution structure of human BCL-w: modulation of ligand binding by the C-terminal helix. J Biol Chem 2003;278: 21124–8.
17. Hinds MG, Lackmann M, Skea GL, Harrison PJ, Huang DC, Day CL. The structure of Bcl-w reveals a role for the C-terminal residues in modulating biological activity. EMBO J 2003;22:1497–507.
18. McDonnell JM, Fushman D, Milliman CL, Korsmeyer SJ, Cowburn D. Solution structure of the proapoptotic molecule BID: a structural basis for apoptotic agonists and antagonists. Cell 1999;96:625–34.
19. Chou JJ, Li H, Salvesen GS, Yuan J, Wagner G. Solution structure of BID, an intracellular amplifier of apoptotic signaling. Cell 1999;96:615–24.
20. Klasa RJ, Gillum AM, Klem RE, Frankel SR. Oblimersen Bcl-2 antisense: facilitating apoptosis in anticancer treatment. Antisense Nucleic Acid Drug Dev 2002;12:193–213.
21. Wang JL, Liu DX, Zhang ZJ, et al. Structure-based discovery of an organic compound that binds Bcl-2 protein and induces apoptosis of tumor cells. Proc Natl Acad Sci U S A 2000;97:7124–9.
22. Tzung SP, Kim KM, Basanez G, et al. Antimycin A mimics a cell-death-inducing Bcl-2 homology domain 3. Nat Cell Biol 2001;3:183–91.
23. Becattini B, Sareth S, Zhai D, et al. Targeting apoptosis via chemical design: inhibition of bid-induced cell death by small organic molecules. Chem Biol 2004; 11:1107–17.
24. Enyedy IJ, Ling Y, Nacro K, et al. Discovery of small-molecule inhibitors of Bcl-2 through structure-based computer screening. J Med Chem 2001;44:4313–24.
25. Walensky LD, Kung AL, Escher I, et al. Activation of apoptosis *in vivo* by a hydrocarbon-stapled BH3 helix. Science 2004;305:1466–70.
26. Shiau CW, Yang CC, Kulp SK, Chen KF, Chen CS, Huang JW. Thiazolidenediones mediate apoptosis in prostate cancer cells in part through inhibition of Bcl-xL/Bcl-2 functions independently of PPARγ. Cancer Res 2005;65:1561–9.
27. Oltersdorf T, Elmore SW, Shoemaker AR, et al. An inhibitor of Bcl-2 family proteins induces regression of solid tumors. Nature 2005;435:677–81.
28. Ben-Ezra JM, Kornstein MJ, Grimes MM, Krystal G. Small cell carcinomas of the lung express the bcl-2 protein. Am J Pathol 1994;145:1036–40.
29. Olopade OI, Adeyanju MO, Safa AR, et al. Overexpression of BCL-x protein in primary breast cancer is associated with high tumor grade and nodal metastases. Cancer J Sci Am 1997;3:230–7.
30. Amundson SA, Myers TG, Scudiero D, Kitada S, Reed JC, Fornace AJ. An informatics approach identifying markers of chemosensitivity in human cancer cell lines. Cancer Res 2000;60:6101–10.
31. Simonian PL, Grillot DA, Nunez G. Bcl-2 and Bcl-XL can differentially block chemotherapy-induced cell death. Blood 1997;90:1208–16.
32. Fennell DA, Corbo MV, Dean NM, Monia BP, Cotter FE. *In vivo* suppression of Bcl-X-L expression facilitates chemotherapy-induced leukaemia cell death in a SCID/NOD-Hu model. Br J Haematol 2001;112:706–13.
33. Wendt MD, Shen W, Kunzer A. et al. Discovery and structure-activity relationship of antagonists of B-cell lymphoma 2 family proteins with chemopotentiation activity *in vitro* and *in vivo*. J Med Chem 2006; 49:1165–81.
34. Zhang HC, Nimmer P, Rosenberg SH, Ng SC, Joseph M. Development of a high-throughput fluorescence polarization assay for Bcl-x(L). Anal Biochem 2002;307: 70–5.
35. Nunez G, London L, Hockenbery D, Alexander M, McKearn JP, Korsmeyer SJ. Deregulated Bcl-2 gene expression selectively prolongs survival of growth factor-deprived hemopoietic cell lines. J Immunol 1990;144:3602–10.
36. Milas L, Milas MM, Mason KA. Combination of taxanes with radiation: preclinical studies. Semin Radiat Oncol 1999;9:12–26.
37. Harper JD, Rao PN, John PC. The mitosis-specific monoclonal antibody MPM-2 recognizes phosphoproteins associated with the nuclear envelope in

Chlamydomonas reinhardtii cells. Eur J Cell Biol 1990; 51:272–8.
38. Lai R, Arber DA, Chang KL, Wilson CS, Weiss LM. Frequency of bcl-2 expression in non-Hodgkin's lymphoma: a study of 778 cases with comparison of marginal zone lymphoma and monocytoid B-cell hyperplasia. Mod Pathol 1998;11:864–9.
39. Sinicrope FA, Hart J, Michelassi F, Lee JJ. Prognostic value of bcl-2 oncoprotein expression in stage II colon carcinoma. Clin Cancer Res 1995;1:1103–10.
40. McDonnell TJ, Troncoso P, Brisbay SM, et al. Expression of the proto-oncogene bcl-2 in the prostate and its association with emergence of androgen-independent prostate cancer. Cancer Res 1992;52: 6940–4.
41. Pratt MAC, Krajewski S, Menard M, Krajewska M, Macleod H, Reed JC. Estrogen withdrawal-induced human breast cancer tumour regression in nude mice is prevented by Bcl-2. FEBS Lett 1998;440:403–8.
42. Reed JC. Bcl-2 family proteins: regulators of chemoresistance in cancer. Toxicol Lett 1995;82/83:155–8.
43. Schmitt CA, Lowe SW. Bcl-2 mediates chemoresistance in matched pairs of primary E mu-myc lymphomas *in vivo*. Blood Cells Mol Dis 2001;27:206–16.
44. O'Connor PM, Jackman J, Bae I, et al. Characterization of the p53 tumor suppressor pathway in cell lines of the National Cancer Institute anticancer drug screen and correlations with the growth-inhibitory potency of 123 anticancer agents. Cancer Res 1997;57:4285–300.
45. Developmental Therapeutics Program NCI/NIH. Available from: http://dtp.nci.nih.gov/.
46. Tan TT, Degenhardt K, Nelson DA, et al. Key roles of BIM-driven apoptosis in epithelial tumors and rational chemotherapy. Cancer Cell 2005;7:227–38.
47. Scatena CD, Stewart ZA, Mays D, et al. Mitotic phosphorylation of Bcl-2 during normal cell cycle progression and Taxol-induced growth arrest. J Biol Chem 1998;273:30777–84.
48. Pathan N, Aime-sempe C, Kitada S, Haldar S, Reed JC. Microtubule-targeting drugs induce Bcl-2 phosphorylation and association with Pin1. Neoplasia 2001;3:70–9.
49. Poruchynsky MS, Wang EE, Rudin CM, Blagosklonny MV, Fojo T. Bcl-xL is phosphorylated in malignant cells following microtubule disruption. Cancer Res 1998;58: 3331–8.
50. Fang G, Chang BS, Kim CN, Perkins C, Thompson CB, Bhalla KN. "Loop" domain is necessary for taxol-induced mobility shift and phosphorylation of Bcl-2 as well as for inhibiting taxol-induced cytosolic accumulation of cytochrome *c* and apoptosis. Cancer Res 1998;58: 3202–8.

A Small-Molecule Inhibitor of Bcl-X_L Potentiates the Activity of Cytotoxic Drugs *In vitro* and *In vivo*

Alex R. Shoemaker, Anatol Oleksijew, Joy Bauch, et al.

Cancer Res 2006;66:8731-8739.